Patterned Growth and Field-Emission Properties of AlN Nanocones

Ning Liu,[†] Qiang Wu,*[,†] Chengyu He,[†] Haisheng Tao,[†] Xizhang Wang,[†] Wei Lei,[‡] and Zheng Hu*[,†]

Key Laboratory of Mesoscopic Chemistry of MOE, School of Chemistry and Chemical Engineering, Nanjing University, Nanjing 210093, China, and School of Electronic Science and Engineering, Southeast University, Nanjing 210096, China

ABSTRACT Patterned growth of AlN nanocones on a Ni-coated Si substrate is demonstrated through the reaction between $AlCl_3$ and NH_3 at 700 °C with Mo grid as a mask. The AlN nanocones are selectively deposited in the hollow region of the mask with diameters of ~10 nm at the tips and 50−60 nm at the roots. The field-emission (FE) performance is effectively enhanced by the patterned growth mainly because of the decreased screening effect, and both turn-on and threshold fields are dramatically decreased, less than half of the corresponding ones for the unpatterned product with similar sizes. The results indicate that patterned growth is an efficient and reproducible way to enhance the FE performance of AlN nanocones, which could be applied to optimize the FE properties of other nanoscale field emitters.

KEYWORDS: one-dimensional nanostructure • aluminum nitride • field emission • patterned growth

1. INTRODUCTION

Cold cathode materials have promising applications in military and domestic industries, and now the related researches are focused on application in a field-emission (FE) flat-panel display (1). The evolution of cold cathodes started with Spindt-type field-emitter arrays such as Mo and Si microtips in the late 1960s. The subuliform microtips are ideal morphologies for FE because of the strong local electric field at the tips and the unique direction of electron emission. Because of the expensive and complicated fabrication technique as well as the large surface work function of Mo and Si microtips, they have not been successfully put into practice. Soon after that, diamond and diamondlike carbon films received much attention, which are regarded as good candidates for cold cathodes owing to the low surface electron affinity, high chemical stability, and thermal conductivity. However, the field emitters in these films are randomly oriented and divergence of the emission electrons is unfavorable for the addressable fabrication, which limits their applications (1, 2). Currently, one-dimensional (1D) nanostructures, represented by carbon nanotubes, have attracted increasing interest for their sharp apexes and large aspect ratios, which could efficiently enlarge the enhancement factor for FE. In seeking appropriate materials, low surface work function or electron affinity, high stability, and excellent thermal conductivity are the main guidelines.

AlN is well-known for its small (even negative) electron affinity, high stability, and superior thermal conductivity (3, 4). Recently, various 1D AlN nanostructures such as nanotubes (5−7), nanowires (8), nanobelts (9) and nanocones (10−13) have been synthesized. Among them, AlN nanocone arrays exhibit good FE properties because of their sharp apexes, large aspect ratios, and good alignment on the substrate (10−13). To further improve the FE properties, two means are worth attempting. One is doping other elements such as Si (14) to increase the electron concentration, and the other is adjusting the nanocone density to decrease the screening effect. As experimentally and theoretically confirmed by Nilsson et al., an interemitter distance of about 2 times the height of the 1D nanostructures optimizes the emitted current per unit area (15). Hence, the density of the AlN nanocones plays a crucial role for their FE properties. Screening effects would reduce the field enhancement factor and thus the emission current when the density of the AlN nanocones is high, just like most cases reported (16). Patterned growth is a good method to control the density of the nanostructures, and there are mainly two routes. One is to construct the patterned substrate through selective modification of the surface hydrophilic/hydrophobic nature via, e.g., electron beam lithography, ultraviolet light irradiation, or etching, which could influence the deposition location. The other is to construct the patterned catalyst for the sequential patterned growth of nanostructures (17−19). Because AlN nanostructures can deposit on various substrates without the assistant of a catalyst (10, 20, 21), these two routes are impracticable for the patterned growth of 1D AlN nanostrutures. In this study, patterned growth of AlN nanocones is realized by introducing Mo grid as a mask, which could result in the locatable deposition of AlN nanocones in the hollow region of the mask. The patterned AlN

* To whom correspondence should be addressed. E-mail: wqchem@nju.edu.cn (Q.W.), zhenghu@nju.edu.cn. (Z.H.). Tel.: 0086-25-83686015. Fax: 0086-25-83686251.

Received for review May 15, 2009 and accepted August 3, 2009

[†] Nanjing University.

[‡] Southeast University.

DOI: 10.1021/am9003304

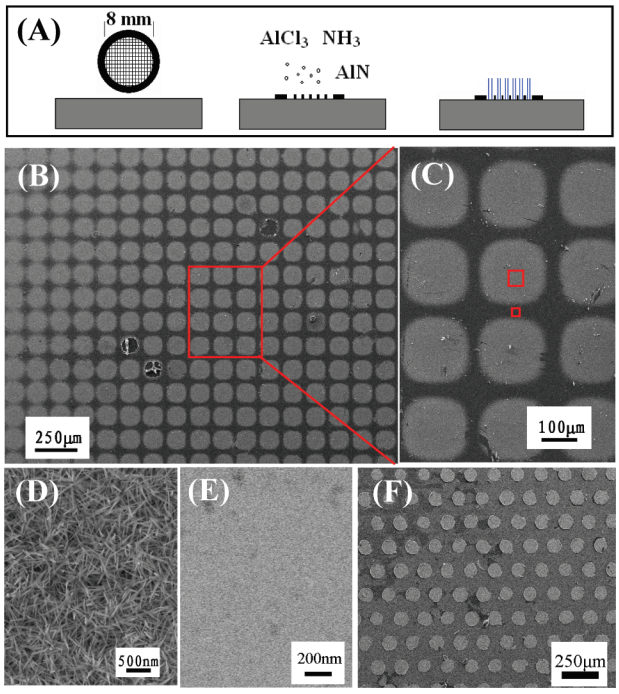

FIGURE 1. Schematic illustration for the patterned growth process (A) and SEM images of the patterned AlN nanocones synthesized using two masks with different pore sizes and gaps (B−F). Patterned sample I: the overview (B), the enlarged region (C), and the part inside the block (D) and in between the neighboring blocks (E) as marked by the panes in part C. Patterned sample II: the overview (F). Compared with pattern I, pattern II has a smaller block size and a larger gap between two neighboring blocks.

nanocones show a much better FE performance in comparison with the unpatterned sample, indicating potential applications.

2. EXPERIMENTAL SECTION

Preparation of Patterned AlN Nanocones. Patterned AlN nanocones were prepared through the reaction between $AlCl_3$ vapor and NH_3 gas at 700 °C (10) under the restriction of a Mo mask, as schematically illustrated in Figure 1A. Briefly, a Mo grid was tightly attached to a Si(111) substrate coated with a 10 nm Ni film. The substrate was placed in the center of an alumina tube in a horizontal tubular furnace. When the temperature was raised to 700 °C, $AlCl_3$ was vaporized upstream at 135 °C and subsequently transported to the reaction zone by an Ar flow (300 sccm), where it reacted with NH_3 gas (20 sccm). AlN nanocones were deposited onto the interspaces of the Mo grid, and the places covered by the Mo cross-bars were bare. The reaction lasted for 4 h, and then the system was cooled down to room temperature under an Ar flow. After removal of the Mo grid, patterned AlN nanocones were obtained. In this paper, two Mo grids with different dimensions have been attempted. For comparison, a Si wafer without a Mo grid was also used as the substrate to deposit AlN products under a similar growth process.

Characterization of the Product. The as-prepared products were characterized by X-ray diffraction (XRD; Philips X'pert Pro X-ray diffractometer) and scanning electron microscopy (SEM; Hitachi S-4800). FE measurements were performed by using a parallel-plate configuration in a vacuum chamber at a pressure of about 1×10^{-4} Pa.

3. RESULTS AND DISCUSSION

SEM images of the patterned AlN nanocones synthesized using two masks with different pore sizes and gaps (patterns I and II) are shown in Figure 1B−F. For the patterned sample I, the dimension of each deposited unit is about 185 μm and the distance between the two neighboring regions is about 35 μm, in good agreement with the pattern of the Mo grid used. The AlN nanocones inside the block show the quasi-aligned morphologies (Figure 1D), while no AlN nanocones could be observed for the place in between the blocks (Figure 1E), which was covered by the grid cross-bar during the synthesis. Compared with the patterned sample I, the patterned sample II has smaller dimension of about 100 μm for each block and a larger distance between two neighboring blocks of about 60 μm (Figures 1F and S1 in the Supporting Information). The patterned products are quite uniform (Figure 1B,F), which favors application as patterned pixels for FE. The AlN nanocones vary from submicrometer to micrometer in length, with diameters of ~10 nm at the tips and 50−60 nm at the roots (see Figure S2 in the Supporting Information). The corresponding energy-dispersive X-ray analysis (EDX; see Figure S3 in the Supporting Information) shows that the atomic ratio of Al to N is about 1:0.93, rather near the stoichiometric ratio of AlN.

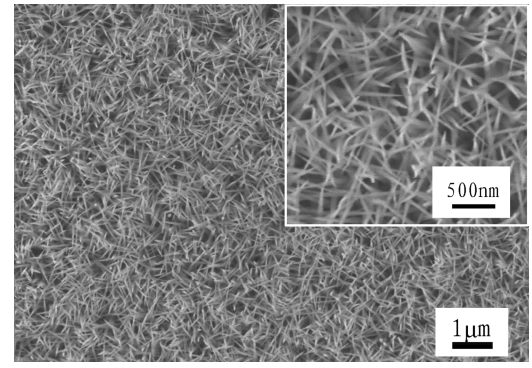

FIGURE 2. SEM images of unpatterned AlN nanocones. The inset shows the magnified image.

Figure 2 shows the SEM images of the unpatterned AlN product without restriction of the Mo grid. The nanocones are quasi-aligned and uniform with geometrical parameters similar to those of the patterned AlN nanocones, indicating the little influence of the Mo mask on the morphology of the AlN nanocones. The XRD curve is in agreement with that of hexagonal AlN (see Figure S4 in the Supporting Information). The growth of the AlN nanocones could be understood as the vapor−solid epitaxial mechanism, as proposed in our previous report (10).

In comparison with the unpatterned AlN nanocones, there exists a larger marginal area for the patterned samples and a better FE performance could be expected because of the enhanced field strength at the marginal region (22). Figure 3A depicts the FE curves of the current density versus the applied field (J−E) for the two patterned and one unpatterned AlN nanocones with a cathode−anode spacing of 100 μm. The turn-on electric field E_{to} (the electric field to generate an emission current density of 10 μA/cm^2) and the threshold field E_{thr} (the electric field to generate an emission current density of 1 mA/cm^2 (23), which could satisfy the primary requirement for application in conventional flat-panel displays) are listed in Table 1. It is seen that both E_{to}

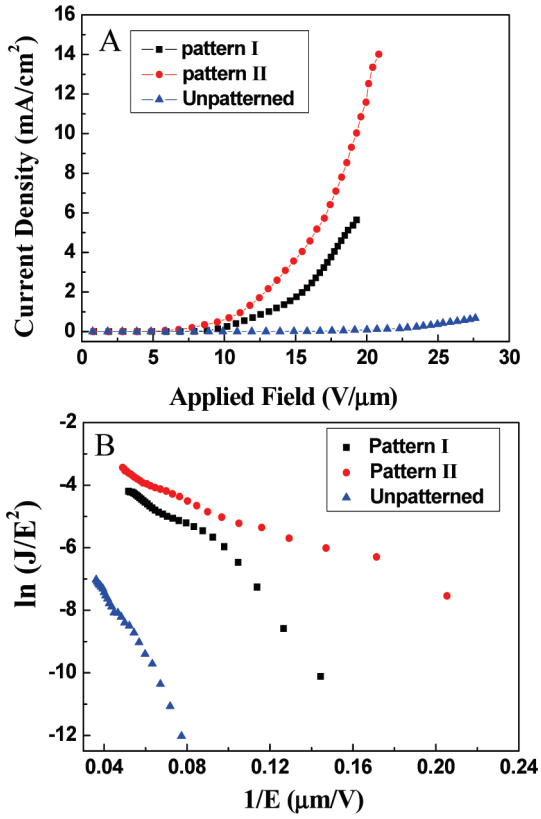

FIGURE 3. (A) $J-E$ curves of the patterned and unpatterned AlN nanocones with an electrode distance of 100 μm. (B) F−N plots corresponding to the $J-E$ curves in part A.

Table 1. E_{to}, E_{thr}, and β of the Patterned and Unpatterned AlN Nanocones

	pattern I	pattern II	unpatterned
E_{to} (V/μm)	7.7	4.8	15.2
E_{thr} (V/μm)	13.1	11.2	29.5
β	977/552	1561	436

and E_{thr} of the two patterned AlN nanocones are lower than half of the corresponding ones of the unpatterned AlN nanocones. Moreover, for the two patterned samples, E_{to} and E_{thr} for the patterned sample II are smaller than the corresponding ones for the patterned sample I. Taking into account the fact that pattern II has a smaller block size and a larger gap between two neighboring blocks than pattern I does, it could be deduced that the enhanced FE of the patterned sample is mainly attributed to the decreased screening effect at the edge of the blocks. This is also supported by the FE images of the patterned AlN array (see Figure S5 in the Supporting Information). Although some other factors such as the shape, defect, impurity, or surface property of the nanocones near the edges could also influence the FE performance of AlN patterns, they could not be the main reason responsible for such a significant increase of the FE properties because all of the samples were synthesized under the same experimental conditions except for the pattern sizes. Hence, the most obvious difference for the three samples is the degree of the screening effect, which should be the dominant factor responsible for their different FE performances. It is seen that the E_{thr} values are still higher than those of carbon nanotubes (24); they are comparable to those of ZnO (25) and B (26) nanowire arrays. These results clearly indicate that patterned growth is an efficient and reproducible method (see Figure S6 in the Supporting Information) to enhance the FE of AlN nanocones mainly because of the decreased screening effect.

The Fowler−Nordheim (F−N) plots of the $J-E$ curves, i.e., $\ln(J/E^2)$ vs $1/E$, are shown in Figure 3B. According to the F−N theory, the slope of the F−N plots is equal to $-6830\phi^{3/2}/\beta$, where ϕ is the work function and β the enhancement factor. Taking $\phi = 3.7$ eV for AlN (6), β is estimated to be 430 for the unpatterned AlN nanocones. As shown in Table 1, the enhancement factors of the two patterned AlN nanocones are increased because of the decreased screening effect. For the patterned sample I, the F−N plots show a two-sectional feature, and β is calculated to be ∼950 and ∼600 at high and low electric fields, respectively. The two-sectional feature of the F−N plot may result from the space charge effect (27). As is deduced from Figure 3A, at least a 5 times larger current density was obtained for the patterned sample I than that for the unpatterned sample at high electric field. The high current density may generate the space charge by ionizing the trace gas molecules existing in the gap, which include the residual gases, the gases desorbed from the anode due to the electron bombardment, and those from the cathode due to local heating. With the positive ions forced to the AlN emitter, the local electric field on the surface of the emitter would be further enhanced, resulting in a larger β value at high electric field. For the patterned sample II, the F−N plot is close to linear and the β value is as high as 1561. This may result from the appearance of the space charge effect even at low electric field because of the fast increase of the current density, as seen in Figure 3A. Hence, the space charge effect functions almost in the whole range of the applied field, different from the case for the patterned sample I, leading to the linear feature of the F−N plot. More direct experimental evidence seems to be needed to clarify this point, e.g., by monitoring the evolution of the space charge distribution with the applied field.

After FE measurements, no obvious morphological change could be observed for the AlN nanocones, which is much different from the case for ZnO nanowire arrays (see Figure S7 in the Supporting Information) (16). This could be attributed to the good flexibility and high stability of AlN nanocones (28), which facilitates the FE application of AlN nanocones.

4. CONCLUSIONS

In summary, a simple route has been developed to prepare patterned AlN nanocones on a Ni-coated Si substrate through the reaction of $AlCl_3$ and NH_3 at 700 °C with Mo grid as a mask. The AlN nanocones have diameters of ∼10 nm at the tips and 50−60 nm at the roots. The patterned growth could effectively decrease the screening effect because of the increased marginal region. As a result, both E_{to} and E_{thr} for the patterned AlN nanocones are dramatically decreased, less than half of the corresponding ones for the unpatterned AlN nanocones. The results indicate that pat-

terned growth is an efficient approach to enhancing the FE properties of AlN nanocones, which should be applicable to optimization of the FE properties of other nanoscale field emitters.

Acknowledgment. This work was jointly supported by the National Basic Research Program of China (2007CB935503), NSFC (Grants 20525312, 20601013, 20873057, and 20833002), and the program for Changjiang Scholars and Innovative Research Team in University.

Supporting Information Available: Figures giving additional SEM images, an XRD pattern, EDX results, and FE measurements. This material is available free of charge via the Internet at http://pubs.acs.org.

REFERENCES AND NOTES

(1) Xu, N. S.; Huq, S. E. *Mater. Sci. Eng. R* **2005**, *48*, 47–189.
(2) Xu, N. S.; Latham, R. V.; Tzeng, Y. *Electron. Lett.* **1993**, *29*, 1596–1597.
(3) Wu, C. I.; Kahn, A.; Hellman, E. S.; Buchanan, D. N. E. *Appl. Phys. Lett.* **1998**, *73*, 1346–1348.
(4) Benjamin, M. C.; Wang, C.; Davis, R. F.; Nemanich, R. J. *Appl. Phys. Lett.* **1994**, *64*, 3288–3290.
(5) Wu, Q.; Hu, Z.; Wang, X. Z.; Lu, Y. N.; Chen, X.; Xu, H.; Chen, Y. *J. Am. Chem. Soc.* **2003**, *125*, 10176–10177.
(6) Tondare, V. N.; Balasubramanian, C.; Shende, S. V.; Joag, D. S.; Godbole, V. P.; Bhoraskar, S. V.; Bhadbhade, M. *Appl. Phys. Lett.* **2002**, *80*, 4813–4815.
(7) Yin, L. W.; Bando, Y.; Zhu, Y. C.; Golberg, D.; Li, M. S. *Adv. Mater.* **2004**, *16*, 929–933.
(8) Wu, Q.; Hu, Z.; Wang, X. Z.; Lu, Y. N.; Huo, K. F.; Deng, S. Z.; Xu, N. S.; Shen, B.; Zhang, R.; Chen, Y. *J. Mater. Chem.* **2003**, *13*, 2024–2027.
(9) Wu, Q.; Hu, Z.; Wang, X. Z.; Chen, Y.; Lu, Y. N. *J. Phys. Chem. B* **2003**, *107*, 9726–9729.
(10) Liu, C.; Hu, Z.; Wu, Q.; Wang, X. Z.; Chen, Y.; Sang, H.; Zhu, J. M.; Deng, S. Z.; Xu, N. S. *J. Am. Chem. Soc.* **2005**, *127*, 1318–1322.
(11) Shi, S. C.; Chen, C. F.; Chattopadhyay, S.; Chen, K. H.; Chen, L. C. *Appl. Phys. Lett.* **2005**, *87*, 073109.
(12) Zhao, Q.; Xu, J.; Xu, X. Y.; Wang, Z.; Yu, D. P. *Appl. Phys. Lett.* **2004**, *85*, 5331–5333.
(13) Tang, Y. B.; Cong, H. T.; Chen, Z. G.; Cheng, H. M. *Appl. Phys. Lett.* **2005**, *86*, 233104.
(14) Tang, Y. B.; Cong, H. T.; Wang, Z. M.; Cheng, H. M. *Appl. Phys. Lett.* **2006**, *89*, 253112.
(15) Nilsson, L.; Groening, O.; Emmenegger, C.; Kuettel, O.; Schaller, E.; Schlapbach, L.; Kind, H.; Bonard, J. M.; Kern, K. *Appl. Phys. Lett.* **2000**, *76*, 2071–2073.
(16) Wang, X. D.; Zhou, J.; Lao, C. S.; Song, J. H.; Xu, N. S.; Wang, Z. L. *Adv. Mater.* **2007**, *19*, 1627–1631.
(17) Weintraub, B.; Deng, Y. L.; Wang, Z. L. *J. Phys. Chem. C* **2007**, *111*, 10162–10165.
(18) Masuda, Y.; Kinoshita, N.; Sato, F.; Koumoto, K. *Cryst. Growth Des.* **2006**, *6*, 75–78.
(19) He, J. H.; Hsu, J. H.; Wang, C. W.; Lin, H. N.; Chen, L. J.; Wang, Z. L. *J. Phys. Chem. B* **2006**, *110*, 50–53.
(20) Shi, S. C.; Chen, C. F.; Chattopadhyay, S.; Lan, Z. H.; Chen, K. H.; Chen, L. C. *Adv. Funct. Mater.* **2005**, *15*, 781–786.
(21) Yazdi, G. R.; Syvajarvi, M.; Yakimova, R. *Appl. Phys. Lett.* **2007**, *90*, 123103.
(22) Di, Y. S.; Yang, X. X.; Lei, W.; Zhang, X. B.; Cui, Y. K.; Wang, Q. L.; Yang, G. D. *Nanotechnology* **2007**, *18*, 505701.
(23) Wang, Q. H.; Corrigan, T. D.; Dai, J. Y.; Chang, R. P. H.; Krauss, A. R. *Appl. Phys. Lett.* **1997**, *70*, 3308–3310.
(24) Fan, S. S.; Chapline, M. G.; Franklin, N. R.; Tombler, T. W.; Cassell, A. M.; Dai, H. J. *Science* **1999**, *283*, 512–514.
(25) Lee, C. J.; Lee, T. J.; Lyu, S. C.; Zhang, Y.; Ruh, H.; Lee, H. J. *Appl. Phys. Lett.* **2002**, *81*, 3648–3650.
(26) Liu, F.; Tian, J. F.; Bao, L. H.; Yang, T. Z.; Shen, C. M.; Lai, X. Y.; Xiao, Z. M.; Xie, W. G.; Deng, S. Z.; Chen, J.; She, J. C.; Xu, N. S.; Gao, H. J. *Adv. Mater.* **2008**, *20*, 2609–2615.
(27) Xu, N. S.; Chen, Y.; Deng, S. Z.; Chen, J.; Ma, X. C.; Wang, E. G. *J. Phys. D: Appl. Phys.* **2001**, *34*, 1597–1601.
(28) Zhang, Y. J.; Liu, J.; He, R. R.; Zhang, Q.; Zhang, X. Z.; Zhu, J. *Chem. Mater.* **2001**, *13*, 3899–3905.

AM9003304